Journal of Nuclear Medicine, published on August 30, 2018 as doi:10.2967/jnumed.118.213140

Antibody-based in vivo PET imaging detects amyloid-β reduction in Alzheimer transgenic mice after BACE-1 inhibition

Running title: ImmunoPET after BACE-1 inhibition

Silvio R Meier[1], Stina Syvänen[1], Greta Hultqvist[2], Xiaotian T Fang[1], Sahar Roshanbin[1], Lars Lannfelt[1,3], Ulf Neumann[4], Dag Sehlin[1]

[1] Department of Public Health and Caring Sciences / Geriatrics, Uppsala University, Dag Hammarskjölds väg 20, 751 85 Uppsala, Sweden

[2] Department of Pharmaceutical biosciences, Uppsala University, Husargatan 3, 751 24 Uppsala, Sweden

[3] BioArctic AB, Warfvinges väg 35, 112 51 Stockholm

[4] Neuroscience Research, Novartis Institutes for BioMedical Research, 4002 Basel, Switzerland

Corresponding author:

Dag Sehlin

Address as above

Telephone: +46184715038

Email: dag.sehlin@pubcare.uu.se

First author:

Silvio R Meier, PhD student

Address as above

Telephone: +46184715038

Email: silvio.meier@pubcare.uu.se

Word count: 4940

Abstract

Positron emission tomography (PET) used for visualizing amyloid-β (Aβ) pathology has become an important tool for specific clinical diagnosis of Alzheimer's disease (AD). However, all available amyloid PET radioligands, such as [^{11}C]PiB, reflect levels of insoluble Aβ plaques, but do not capture soluble and protofibrillar Aβ forms. When measured with current PET ligands, the plaque load appears to be fairly static during clinical stages of AD, and may not be affected by Aβ reducing treatments. The aim of the present study was to investigate if a novel PET radioligand, based on an antibody directed towards soluble aggregates of Aβ, could be used to detect changes in Aβ levels during disease progression and after treatment with a β-secretase (BACE-1) inhibitor.

Methods: One set of transgenic mice (tg-ArcSwe, model of Aβ pathology) aged between 7 and 16 months were PET scanned with the Aβ protofibril selective radioligand [^{124}I]RmAb158-scFv8D3 to follow progression of Aβ pathology in the brain. A second set of tg-ArcSwe mice, aged 10 months, were treated with BACE-1 inhibitor NB-360 for 3 months and compared to an untreated control group. A set of 10 months old tg-ArcSwe mice also underwent PET scanning, acting as a baseline group. Brain tissue was isolated after PET to determine levels of Aβ by ELISA and immunohistochemistry.

Results: Concentration of [^{124}I]RmAb158-scFv8D3 in tg-ArcSwe mice, measured *in vivo* with PET, increased with age and corresponded well with *ex vivo* autoradiography and Aβ immunohistochemistry. Tg-ArcSwe mice treated with NB-360 showed significantly lower *in vivo* PET signals than untreated animals, and were similar to the baseline 10 month old animals. The decreased [^{124}I]RmAb158-scFv8D3 concentrations in NB-360 treated mice, quantified with PET, corresponded well with decreased Aβ levels measured in *post mortem* brain.

Conclusion: A number of treatments for AD are currently studied in phase 2 and 3 clinical trials but there are limited possibilities to study their effects on the important, non-fibrillar Aβ forms *in vivo*. This study

demonstrates the ability of the Aβ protofibril selective radioligand [^{124}I]RmAb158-scFv8D3 to follow disease progression and detect treatment effects with PET imaging in tg-ArcSwe mice.

Keywords (3-5): Alzheimer's disease; positron emission tomography (PET); antibody-based radioligand; BACE-1 inhibitor NB-360; amyloid-β

Introduction

Alzheimer´s disease (AD) is the most common neurodegenerative disease and the number of people affected will increase as a consequence of an ageing population. However, there is no treatment available that halts the pathological changes underlying disease progression. The amyloid hypothesis[1] states that aggregation of the amyloid-beta (Aβ) protein eventually leads to neurodegeneration and finally to dementia. To reduce Aβ pathology, immunotherapy studies have been conducted with several Aβ antibodies[2]. Aducanumab, which targets Aβ aggregates, recently showed beneficial effects in AD patients[3] and BAN2401[4], the humanized version of mAb158[5,6] that targets soluble Aβ protofibrils, is currently studied in a phase 2b clinical trial. In addition, a number of low molecular weight β-secretase (BACE-1) inhibitors, aimed to reduce Aβ production, are currently in clinical trials.

Since the pathological Aβ accumulation occurs over many years, it is crucial to have access to sensitive, specific and representative diagnostic tools to follow disease progression and potential effects of disease modifying treatments in clinical studies.

Several small molecular PET ligands such as [^{11}C]PiB or [^{18}F]Fluorbetaben visualize amyloid plaques and have become important tools as AD diagnostics. However, amyloid PET may be positive years before any clinical symptoms are presented[7], and show an early saturation during disease progression[8]. In addition, diagnosis with [^{11}C]PiB and analogues has limited value in cases with diffuse Aβ pathology, as diffuse plaques largely lack the β-sheet fibrillar structure to which these radioligands bind[9]. Studies on Aβ toxicity have indicated that soluble aggregates, e.g. oligomers and protofibrils, are the most neurotoxic Aβ species[10–12]. In addition, brain level of soluble Aβ protofibrils seems to be a more dynamic indicator of disease severity and may thus be a better marker for disease progression than insoluble plaques[8,11]. It is

also likely that novel treatments directed at decreasing Aβ production (β-secretase inhibitors) or enhancing Aβ clearance (immunotherapy) will reduce levels of soluble Aβ before an effect on plaque load can be detected. Treatment effects could thus be difficult to monitor with current amyloid PET tracers. In fact, a recent study found only subtle changes in amyloid with the PET tracer ^{18}F-AV45 in APPPS1-21 mice treated with BACE-1 inhibitor (JNJ-49146981) for 12 months[13]. Hence, a PET radioligand that visualizes other forms than insoluble, fibrillar Aβ could be an important tool for detecting drug effects in clinical trials.

We previously described the radioligand [^{124}I]RmAb158-scFv8D3, which is based on the antibody mAb158, selectively binding to soluble Aβ protofibrils, with moderate and low cross-reactivity to Aβ fibrils and monomers, respectively[6,14,15]. Antibodies, due to their large molecular size, are generally characterized by very limited passage across the blood-brain barrier (BBB). To enhance brain uptake of mAb158 and enable its use as a PET radioligand, it was functionalized with two single chain variable fragments (scFv) of the transferrin receptor (TfR) antibody 8D3[16]. This conjugation leads to active transcytosis via the TfR into the brain[17]. A number of similar constructs[15,18,19] have been used to image the progressive accumulation of soluble Aβ aggregates in AβPP-transgenic mice (tg-ArcSwe[20]) at different ages, demonstrating the potential of bispecific antibodies as neuro PET radioligands.

The aim of the present study was in a first step, to investigate the ability of [^{124}I]RmAb158-scFv8D3 to follow disease progression, i.e. escalating brain Aβ pathology, in the tg-ArcSwe mouse model. This was achieved by comparison of *in vivo* PET with [^{124}I]RmAb158-scFv8D3 in tg-ArcSwe mice of different ages in relation to *ex vivo* measurement of brain radioactivity and Aβ pathology in *post mortem* analyzed brain tissue from the same group of mice.

In a second set of mice, Aβ reduction after treatment with BACE-1 inhibitor NB-360[21] was studied to investigate the ability of [^{124}I]RmAb158-scFv8D3 to image the reverse effect, i.e. a decrease in brain Aβ pathology. In previous studies NB-360 has shown a robust Aβ reduction and promising pharmacokinetic profile in AβPP transgenic mice. In addition, it has demonstrated a beneficial effect on cellular, long-range circuitry and memory in APP23xPS45 transgenic mice[22]. Thus, we conducted a preclinical NB-360 treatment study in tg-ArcSwe mice, designed to resemble a clinical study of a new drug candidate, using [^{124}I]RmAb158-scFv8D3 PET imaging to quantify the treatment effect *in vivo*.

Materials and Methods

Animals

Mice harboring the *Arctic* (AβPP E693G) and the *Swedish* (AβPP KM670/671NL) *AβPP* mutations, tg-ArcSwe[20], were PET scanned to study disease progression at the age of 7, 10, 13 and 16 months. The effect of NB-360 treatment was investigated in mice aged 10 months at the start of the treatment, i.e. at an age characterized by moderate Aβ pathology[23] but no detectable [^{11}C]PIB PET [15]. The number of mice in each age group is displayed in Supplemental Table 1.

Throughout the experiment, animals were kept with free access to food and water in rooms with controlled temperature and humidity in an animal facility at Uppsala University. All experiments described in this project were approved by the Uppsala County Animal Ethics board (#C17/14) following the rules and regulations of the Swedish Animal Welfare Agency and were in compliance with the European Communities Council Directive of 22 September 2010.

Radioligand

The recently described radioligand [^{124}I]RmAb158-scFv8D3 was used for antibody based PET imaging. Its expression and pharmacokinetics are described in Hultqvist et al. 2017[17]. The radioligand is based on the well-studied antibody mAb158, which displays a selective binding to Aβ protofibrils[6,14,15]. To increase the transport of mAb158 across the BBB into the brain, two scFv of the TfR antibody 8D3[16] were attached using short linkers to the C-termini of the light chains of mAb158. This enables monovalent TfR binding, which leads to efficient transcytosis over the BBB. RmAb158-scFv8D3 was recombinantly expressed in Expi293 cells and purified as described previously[17].

Radiochemistry

RmAb158-scFv8D3 was labelled with iodine-124 (^{124}I) using direct radioiodination[24]. Radiolabeling was done in six batches; 119 ± 31.3 MBq ^{124}I solution (Perkin-Elmer Inc.) was pre-incubated 15 min with NaI at a concentration of 10 µM. RmAb158-scFv8D3 was mixed with phosphate buffered saline (PBS) and added to the Iodine solution at 0.6 µg/MBq to a final volume of 380 µl. The reaction was activated by adding 40 µl Chloramine-T solution (1 mg/ml) and quenched after 120 seconds by addition of 80 µl of sodium metabisulfite solution (1 mg/ml). The radiolabeled protein was purified from free iodine and low-molecular weight components with a disposable NAP-5 size exclusion column with a MW cut-off 5 kDa (GE Healthcare AB, Uppsala, Sweden). The high molecular weight fraction containing the labelled protein was eluted with 1 ml PBS.

PET imaging

PET imaging was performed with [^{124}I]RmAb158-scFv8D3 using a Triumph Trimodality System (TriFoil Imaging, Inc., Northridge, CA, USA). To reduce thyroidal uptake of ^{124}I, mice were administered 0.5% NaI in the drinking water one day before radioligand injection and then 0.2% NaI until the PET scan. Mice

included in the disease progression investigation were intravenously (i.v.) injected with 14.8±2.6 MBq [^{124}I]RmAb158-scFv8D3 with a specific activity of 234 MBq/nmol and scanned 4 days post injection. Mice included in the NB-360 treatment experiment were i.v. injected with 7.4±1.3 MBq [^{124}I]RmAb158-scFv8D3 with a specific activity of 161 ± 12.7 MBq/nmol and PET/CT scanned 6 days after injection. Prior to PET scanning, animals were anesthetized with 2.5% isoflurane, moved to the heated scanner bed and kept anesthetized with 1.5-2% isoflurane during the scan. PET scan duration was 60 min followed by a CT examination of 3 min (Field of View (FOV) = 8.0 cm).

Directly after scanning, mice underwent a 2 min intracardiac perfusion with 0.9% NaCl. Brain and blood samples were collected and *ex vivo* radioactivity was measured with a well counter (GE Healthcare, Uppsala, Sweden).

PET data was reconstructed using the ordered subsets expectation-maximization (OSEM) 3D algorithm (20 iterations). CT raw files were reconstructed using Filtered Back Projection (FBP). All subsequent processing of PET and CT images was performed in imaging software Amide 1.0.4[25]. The CT scans were manually aligned with a T2 weighted, MRI based mouse brain atlas[26] containing outlined regions of interest for whole brain, cortex and hippocampus. The PET image was then aligned with the CT and the atlas and PET data could be quantified in regions of interest.

***Ex vivo* autoradiography**

Frozen right hemispheres of [^{125}I]RmAb158-scFv8D3 injected mice were cryosectioned (20 µm) with a LEICA CM 1850 at -25°C. Sections were stored at -20°C until use. Fresh tissue sections were placed in an x-ray cassette and exposed to positron-sensitive phosphor screens (MS, MultiSensitive, PerkinElmer, Downers grove, IL, USA) for 6 days. The plates were then scanned with a Cyclone Plus Imager system (Perkin Elmer) at a resolution of 600 dpi. Images were analyzed by ImageJ 1.51.

NB-360 Treatment

Three groups of mice were investigated (Fig. 1, Supplemental Table 1); the NB-360 treated group was provided food containing BACE-1 inhibitor NB-360 (Novartis, Basel) with a concentration of 0.5 g/kg during 3 months while the vehicle group was maintained on control food until the age of 13 months. Mice from 4 litters were randomly allocated to NB-360 or vehicle treated groups and all mice were studied during the same period. The baseline group, included to provide an estimate of Aβ pathology level before the treatment, had free access to control food until the age of 10 months, when PET scans and analyses were conducted. All groups were scanned at the same occasion. Brains were extracted and pathology was analyzed with immunohistochemistry and immunoassays, as described in the Supplemental Methods.

Statistics

All statistical analyses and graphs were done in GraphPad Prism 6 (GraphPad Software, Inc, La Jolla, CA, USA). Results of groups are reported as mean ± standard deviation. Data was analyzed with one-way ANOVA followed by Bonferroni´s post hoc test.

Results

Tg-ArcSwe mice between 7 and 16 months were PET scanned using [^{124}I]RmAb158-scFv8D3 to study the radioligand's ability to visualize progression of Aβ brain pathology. PET images corresponded well with *ex vivo* autoradiography images of brain sections prepared from perfused brain, i.e. tissue devoid of any background signal from blood (Fig. 2). Aβ40 staining displayed a clear increase of the Aβ burden with age. Further, the overlay of the autoradiography and the Aβ40 staining showed a high degree of co-localization between areas with high Aβ40 pathology and high retention of [^{124}I]RmAb158-scFv8D3 (Fig. 2).

At the age of 7 months, astrocyte activation measured with GFAP immunohistochemistry was very rare and limited to certain spots in cortex. With increasing plaque load at the age of 10 and 13 months, astrocytes were activated around plaques. At the age of 16 months, a comprehensive, area-wide activation could be observed (Fig. 2).

In the second set of mice, PET scans were conducted after 3 months of treatment with NB-360 containing food pellets or control food. A group of younger mice, representing the baseline, were also studied. The [^{124}I]RmAb158-scFV8D3 brain retention in the baseline group and the NB-360 treated group was low and there was no notable difference between these two groups, indicating that Aβ pathology progression was halted by BACE-1 inhibitor treatment. In contrast, the group that had received control food showed a high PET signal in areas of abundant Aβ pathology (Fig. 3).

In line with the *in vivo* results, whole brain Aβ staining revealed higher Aβ burden in the vehicle group compared to the NB-360 and baseline groups. Pathology was observed mainly in cortex, hippocampus and, with further disease progression in the vehicle group, also in thalamus (Fig. 3). Aβ/GFAP double staining of prefrontal cortex showed higher GFAP activity in the vehicle group than NB-360 and baseline. Higher activation could especially be observed around plaques (Fig. 3).

Image-based quantification of radioactivity showed that there was no significant difference in any of the studied regions when comparing the baseline and NB-360 treated groups, whereas the vehicle group showed significantly higher activity in all brain regions, most pronounced in cortex and hippocampus (Fig. 4; $p=0.002$ in whole brain, $p<0.0001$ in cortex and $p<0.0001$ in hippocampus). To verify the PET results, Aβ levels were biochemically assessed with electrochemiluminescence immunoassay (MSD technology) and ELISA in TBS soluble and insoluble brain extracts obtained from the same mice that had undergone

PET. There was no significant difference in TBS-soluble Aβ38, Aβ40 and Aβ42 levels between the NB-360 and baseline group. However, a small trend towards slightly higher levels of all studied Aβ species could be observed in the NB-360 group (Fig. 5 A-C). The vehicle group showed significantly higher levels of soluble Aβ38, Aβ40 and Aβ42 compared to baseline and treated animals ($p=0.0001$, $p=0.0013$ and $p=0.0001$, respectively) (Fig. 5 A-C). Similar results were observed for soluble Aβ aggregates (Fig. 5D), where untreated mice displayed significantly higher levels than treated ($p<0.0001$) and baseline ($p<0.0001$) mice. Here, a trend was observed towards lower levels in the NB-360 group compared with baseline. A ratio of soluble Aβ aggregates over total soluble Aβ displayed a nearly significant difference ($p=0.051$) between baseline (1.9±1.4) and NB-360 (0.8±0.5), indicating a relative decrease in Aβ oligomerization as a result of BACE-1 inhibition.

ELISA analysis of FA soluble brain extracts, which represents total Aβ40 and Aβ42 including plaques, also showed similar results. Aβ levels in baseline and NB-360 treated mice were equally low, indicating a similar plaque load in treated and baseline mice. Again, the vehicle group had significantly higher Aβ levels (for Aβ40 $p<0.0001$ and for Aβ42 $p<0.0001$) (Fig. 5E-F).

Discussion

During the past decade, amyloid PET imaging, using e.g. [^{11}C]PiB, has become an important tool for reliable diagnosis of Aβ plaque pathology. However, while amyloid plaques are a hallmark of AD, soluble Aβ may be a more dynamic marker for disease progression. Moreover, since current drugs in development are mainly aimed to reduce soluble Aβ, existing amyloid PET ligands may not be optimal to quantify effects of treatment. In the present study, we demonstrate that a recombinantly produced PET ligand, derived from the Aβ protofibril selective antibody mAb158, can be used to visualize and quantify the progression of Aβ

pathology in transgenic tg-ArcSwe mice and further, that it detects changes in brain Aβ levels related to an Aβ reducing treatment.

PET imaging requires a certain density of the target in the studied tissue to produce a signal that can be reliably quantified. While brain concentrations of soluble Aβ protofibrils, the target of mAb158, are elevated already at 2 months of age in tg-ArcSwe mice [27], levels are initially very low until plaques start to develop around 6 months[20], catalyzing Aβ aggregation and accumulation of soluble aggregates[28]. Using the novel PET ligand [^{124}I]RmAb158-scFv8D3, Aβ pathology was detected already from the age of 7 months, with a broad dynamic range and an increasing PET signal up to the age of 16 months (Fig. 2 and Supplemental Fig. 1A). PET results correlated well with *ex vivo* measured radioactivity and Aβ pathology (Supplemental Fig. 1B and Fig. 2). This is to compare with [^{11}C]PiB PET imaging, which in a previous study barely detected Aβ pathology at the age of 12 months, but gave detectable signals at 18 months[15], despite the dense, AD-like nature of tg-ArcSwe plaques [23]. [^{11}C]PiB, binding to the amyloid plaque core, thus seems to require a very high density of plaques to produce a signal. In contrast, although dependent on the presence of plaques, [^{124}I]RmAb158-scFv8D3 seems to detect a more dynamic and abundant pool of Aβ, associated with the plaques. Based on these findings, a study was designed to investigate the sensitivity of [^{124}I]RmAb158-scFv8D3 PET to Aβ reducing treatment at an early stage of Aβ pathology.

The reduction of Aβ accumulation in tg-ArcSwe mice was achieved with BACE-1 inhibitor NB-360, which previously gave a prominent Aβ reduction in APP51/16 mice[21]. After three months of treatment, PET images obtained with the Aβ protofibril selective radioligand [^{124}I]RmAb158-scFv8D3 clearly visualized a markedly reduced Aβ pathology in NB-360 treated mice in comparison with the vehicle group, very similar to baseline (Fig. 3). Quantification of PET data confirmed this result, with equally low signals in baseline

and NB-360 treated mice and a significantly higher signal in the vehicle group, especially in brain regions with abundant Aβ pathology, such as cortex and hippocampus (Fig. 4). These results suggest that Aβ accumulation was essentially halted during the three months' treatment and that the PET ligand clearly detected this treatment effect *in vivo* at a stage of pathology that is below the detection limit of [^{11}C]PiB PET imaging in this animal model.

ELISA analyses of TBS brain extracts confirmed PET results. Animals without treatment had a normal development of pathology from the age of 10 to 13 month with a usual range of variation when compared with previous investigations[5,20,23]. In contrast, levels of soluble Aβ aggregates (Fig. 5D), the primary target for [^{124}I]RmAb158-scFv8D3, were 3-fold lower in treated mice compared with their untreated littermates and at a similar level as baseline mice. Similarly, levels of total soluble Aβ38, Aβ40 and Aβ42 were 3-fold reduced in treated animals (Fig. 5A-C), almost to the baseline level, suggesting that BACE-1 inhibition maintained low levels of soluble Aβ but did not induce an overall reduction over time. Interestingly, although not statistically significant (p=0.051), the relative amount of aggregated Aβ in the soluble pool (soluble Aβ aggregates/total soluble Aβ) was lower in the treated group compared to baseline, suggesting that the inhibited Aβ production decreased the rate of aggregation.

As a consequence of reduced production and aggregation, Aβ deposition and plaque formation was halted in NB-360 treated animals. Aβ deposits were detected with Aβ40 immunohistochemistry in prefrontal cortex and hippocampus in the baseline group and did not change over time with NB-360 treatment. However, untreated animals with a normal course of disease reached a significantly higher plaque load during the study (Fig. 3), which was also confirmed by ELISA quantification of total Aβ40 and Aβ42 in FA

soluble brain extracts (Fig. 5E-F). The distinct GFAP staining around plaques seen in the vehicle group was reduced in treated mice, indicating a prominent effect of NB-360 treatment also on neuroinflammation.

Although the decreased plaque load per se could potentially contribute to the reduced PET signal observed here, previous studies with mAb158 derived ligands have shown little correlation between PET signal and insoluble Aβ. In contrast, binding was observed around plaques and there was a good correlation with soluble Aβ protofibrils[15]. Formation of soluble Aβ aggregates has been reported to occur in the area surrounding amyloid plaques[28]. A decreased plaque load thus implies fewer oligomerization sites and a reduction in the formation of plaque associated, protofibrillar Aβ. Such Aβ reduction was previously reported after NB-360 treatment in APP23xPS45 transgenic mice[22]. Here, ELISA analyses of *post mortem* brain revealed an overall reduction in soluble Aβ aggregates after BACE-1 inhibition and notably, a smaller proportion of soluble Aβ seemed to be in an aggregated state. The substantially decreased *in vivo* PET signal observed here is therefore likely to represent this reduction in soluble Aβ aggregates. Altogether, these findings highlight the potential of measuring soluble Aβ aggregates *in vivo* to monitor disease progression and detect effects of Aβ reducing treatment. They may also explain the pronounced difference in PET signal achieved with [^{124}I]RmAb158-scFv8D3 after BACE-1 inhibition, as compared to the modest differences detected with the small molecular PET ligand ^{18}F-AV45[13], which visualizes the dense core of amyloid plaques.

Conclusion

In conclusion, antibody based PET imaging of soluble Aβ protofibrils is a sensitive tool for following progression of brain Aβ pathology and treatment effects achieved by inhibition of Aβ production. This is a

step towards a method that could be used in future preclinical and clinical studies of novel AD drug candidates.

Disclosure

U.N. is employee and shareholder of Novartis Pharma AG, Basel, Switzerland. L.L. is founder and shareholder of BioArctic AB, Stockholm, Sweden. All other authors declare no competing financial interests. Financial support was granted from the Swedish Research Council (#2017-02413), Alzheimerfonden, Hjärnfonden, Torsten Söderbergs stiftelse, Hedlunds stiftelse, Stiftelsen Fondkistan, Åhlén-stiftelsen, Stiftelsen Sigurd och Elsa Goljes minne, Stohnes stiftelse, Stiftelsen för Gamla tjänarinnor, Magnus Bergwalls stiftelse and the Uppsala Berzelii Technology Centre for Neurodiagnostics.

Acknowledgements

We would like to acknowledge Dr. Derya Shimshek, Novartis, for supplying the NB-360 food pellets, Professor Lars Nilsson for developing the mouse model used in this study and BioArctic AB for sharing the mAb158 sequence. The molecular imaging work in this study was performed at SciLifeLab Pilot Facility for Preclinical PET-MRI, a Swedish nationally available imaging platform at Uppsala University, Sweden, financed by Knut and Alice Wallenberg Foundation.

References

1. Hardy, J. A. & Higgins, G. A. Alzheimer's disease: the amyloid cascade hypothesis. *Science* **256,** 184–185 (1992).
2. Hung, S.-Y. & Fu, W.-M. Drug candidates in clinical trials for Alzheimer's disease. *J. Biomed. Sci.* **24,** (2017).
3. Sevigny, J. *et al.* The antibody aducanumab reduces Aβ plaques in Alzheimer's disease. *Nature* **537,** 50–56 (2016).
4. Logovinsky, V. *et al.* Safety and tolerability of BAN2401--a clinical study in Alzheimer's disease with a protofibril selective Aβ antibody. *Alzheimers Res. Ther.* **8,** 14 (2016).
5. Lord, A. *et al.* An amyloid-beta protofibril-selective antibody prevents amyloid formation in a mouse model of Alzheimer's disease. *Neurobiol. Dis.* **36,** 425–434 (2009).
6. Englund, H. *et al.* Sensitive ELISA detection of amyloid-β protofibrils in biological samples. *J. Neurochem.* **103,** 334–345 (2007).
7. Chételat, G. *et al.* Amyloid imaging in cognitively normal individuals, at-risk populations and preclinical Alzheimer's disease. *NeuroImage Clin.* **2,** 356–365 (2013).
8. Engler, H. *et al.* Two-year follow-up of amyloid deposition in patients with Alzheimer's disease. *Brain* **129,** 2856–2866 (2006).
9. Schöll, M. *et al.* Low PiB PET retention in presence of pathologic CSF biomarkers in Arctic APP mutation carriers. *Neurology* **79,** 229–236 (2012).
10. Esparza, T. J. *et al.* Soluble Amyloid-beta Aggregates from Human Alzheimer's Disease Brains. *Sci. Rep.* **6,** 38187 (2016).
11. Esparza, T. J. *et al.* Amyloid-beta oligomerization in Alzheimer dementia versus high-pathology controls. *Ann. Neurol.* **73,** 104–119 (2013).

12. Walsh, D. M. *et al.* Naturally secreted oligomers of amyloid beta protein potently inhibit hippocampal long-term potentiation in vivo. *Nature* **416,** 535–539 (2002).
13. Deleye, S. *et al.* Evaluation of µPET outcome measures to detect disease modification induced by BACE inhibition in a transgenic mouse model of Alzheimer's disease. *J. Nucl. Med. Off. Publ. Soc. Nucl. Med.* (2017). doi:10.2967/jnumed.116.187625
14. Magnusson, K. *et al.* Specific uptake of an amyloid-β protofibril-binding antibody-tracer in AβPP transgenic mouse brain. *J. Alzheimers Dis. JAD* **37,** 29–40 (2013).
15. Sehlin, D. *et al.* Antibody-based PET imaging of amyloid beta in mouse models of Alzheimer's disease. *Nat. Commun.* **7,** 10759 (2016).
16. Kissel, K. *et al.* Immunohistochemical localization of the murine transferrin receptor (TfR) on blood–tissue barriers using a novel anti-TfR monoclonal antibody. *Histochem. Cell Biol.* **110,** 63–72 (1998).
17. Hultqvist, G., Syvänen, S., Fang, X. T., Lannfelt, L. & Sehlin, D. Bivalent Brain Shuttle Increases Antibody Uptake by Monovalent Binding to the Transferrin Receptor. *Theranostics* **7,** 308–318 (2017).
18. Syvänen, S. *et al.* A bispecific Tribody PET radioligand for visualization of amyloid-beta protofibrils - a new concept for neuroimaging. *NeuroImage* **148,** 55–63 (2017).
19. Sehlin, D., Fang, X. T., Meier, S. R., Jansson, M. & Syvänen, S. Pharmacokinetics, biodistribution and brain retention of a bispecific antibody-based PET radioligand for imaging of amyloid-β. *Sci. Rep.* **7,** 17254 (2017).
20. Lord, A. *et al.* The Arctic Alzheimer mutation facilitates early intraneuronal Aβ aggregation and senile plaque formation in transgenic mice. *Neurobiol. Aging* **27,** 67–77 (2006).
21. Neumann, U. *et al.* A novel BACE inhibitor NB-360 shows a superior pharmacological profile and robust reduction of amyloid-β and neuroinflammation in APP transgenic mice. *Mol. Neurodegener.* **10,** 44 (2015).

22. Keskin, A. D. *et al.* BACE inhibition-dependent repair of Alzheimer's pathophysiology. *Proc. Natl. Acad. Sci. U. S. A.* **114,** 8631–8636 (2017).

23. Philipson, O. *et al.* A highly insoluble state of Abeta similar to that of Alzheimer's disease brain is found in Arctic APP transgenic mice. *Neurobiol. Aging* **30,** 1393–1405 (2009).

24. Greenwood, F. C., Hunter, W. M. & Glover, J. S. The preparation of 131I-labelled human growth hormone of high specific radioactivity. *Biochem. J.* **89,** 114–123 (1963).

25. Loening, A. M. & Gambhir, S. S. AMIDE: a free software tool for multimodality medical image analysis. *Mol. Imaging* **2,** 131–137 (2003).

26. Ma, Y. *et al.* A three-dimensional digital atlas database of the adult C57BL/6J mouse brain by magnetic resonance microscopy. *Neuroscience* **135,** 1203–1215 (2005).

27. Lord, A. *et al.* Amyloid-beta protofibril levels correlate with spatial learning in Arctic Alzheimer's disease transgenic mice. *FEBS J.* **276,** 995–1006 (2009).

28. Koffie, R. M. *et al.* Oligomeric amyloid beta associates with postsynaptic densities and correlates with excitatory synapse loss near senile plaques. *Proc. Natl. Acad. Sci. U. S. A.* **106,** 4012–4017 (2009).

Figures

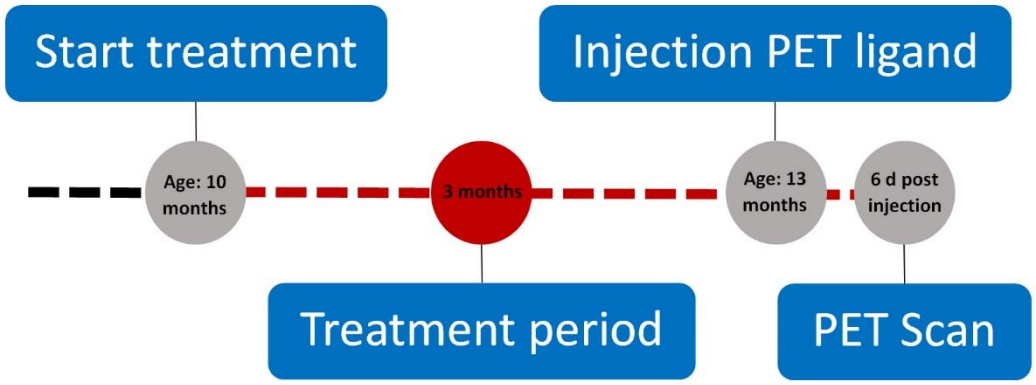

Figure 1: Overview of treatment and PET imaging. At the age of 10 months, animals were given either food containing BACE-1 inhibitor NB-360 or control food. At the age of 13 months, animals were injected with the radioligand and PET scanned 6 days later. A third group was PET scanned and analyzed at the baseline age of 10 months for comparison at the starting point.

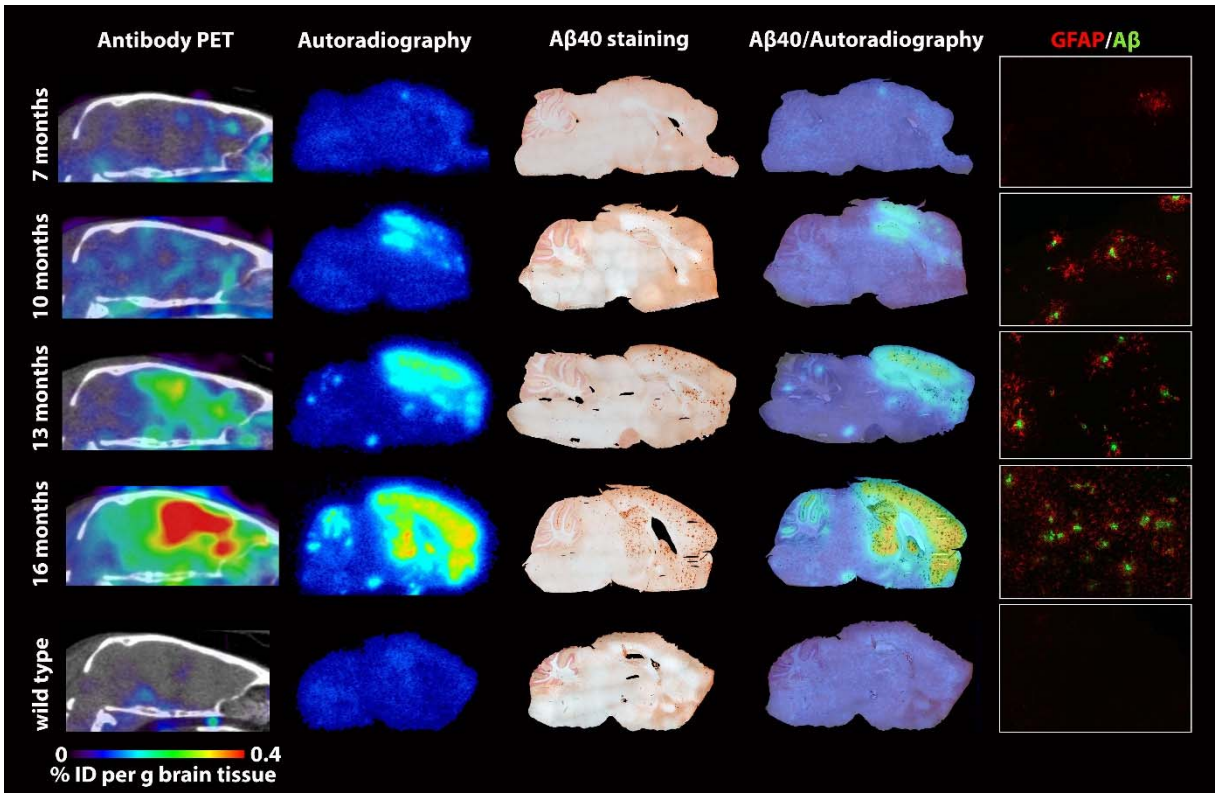

Figure 2: Disease progression and comparison between PET and *ex vivo* analysis. Representative images of disease progression in tg-ArcSwe mice from the age of 7 months up to 16 months. From left to right, *in vivo* PET images with [^{124}I]RmAb158-scFv8D3 are compared to corresponding *ex vivo* autoradiography and Aβ40 staining of the same individual. The overlay of Aβ40 staining and *ex vivo* autoradiography highlights the co-localization of injected [^{124}I]RmAb158-scFv8D3 and Aβ40 pathology. The GFAP/Aβ column shows activated astrocytes around Aβ deposits at 20x magnification in the cortex.

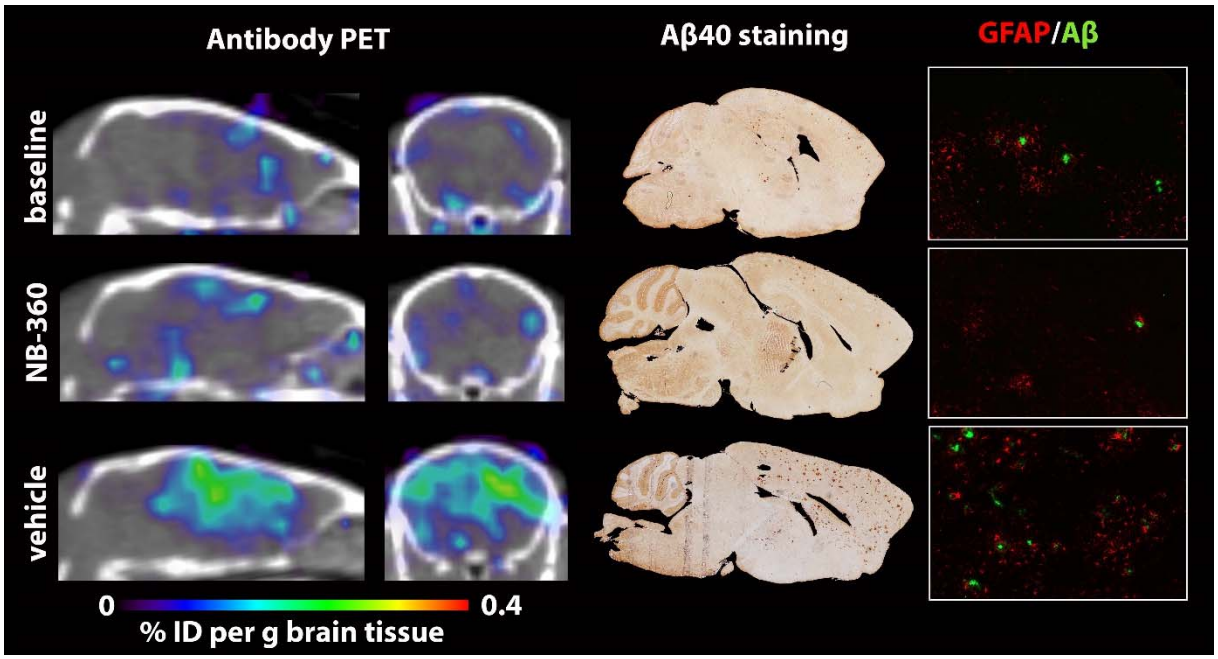

Figure 3: Overview of PET imaging, Aβ and GFAP pathology following NB-360 treatment. Comparison of the three groups of mice – baseline, NB-360 and vehicle. Sagittal and coronal PET images (left), with brain concentrations of [^{124}I]RmAb158-scFv8D3 expressed as % of injected dose (%ID) per gram brain tissue. Corresponding Aβ40 whole brain staining images show total Aβ burden, including plaque pathology (middle). Aβ and GFAP staining demonstrate co-localization of Aβ deposits and reactive astrocytes at 20x magnification (right).

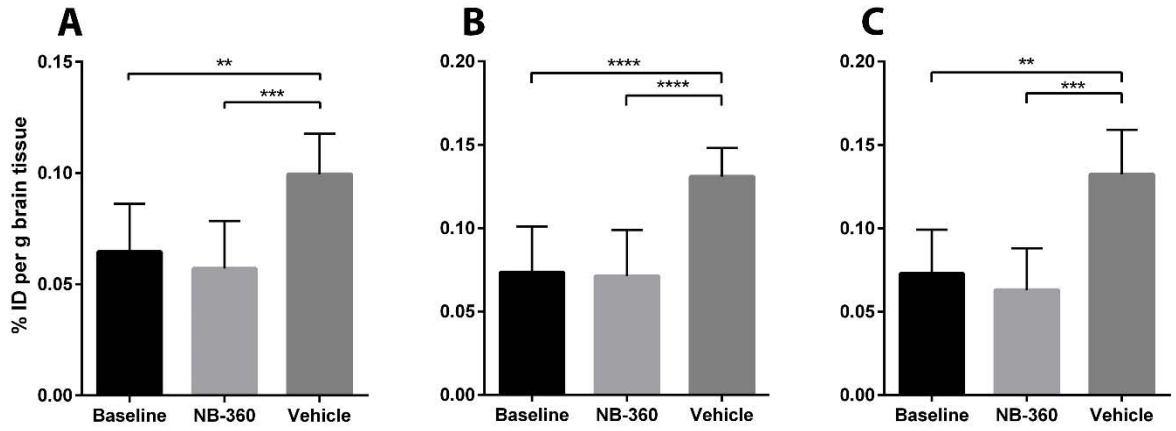

Figure 4: PET quantification of different brain regions. Image-based radioactivity, expressed as %ID per gram brain tissue, of whole brain (**A**), cortex (**B**) and hippocampus (**C**). While there was no significant difference between baseline and NB-360, the vehicle group showed significantly higher activity in all brain regions ($p=0.002$ in whole brain, $p<0.0001$ in cortex and $p<0.0001$ in hippocampus). Values represent group mean with standard deviation.

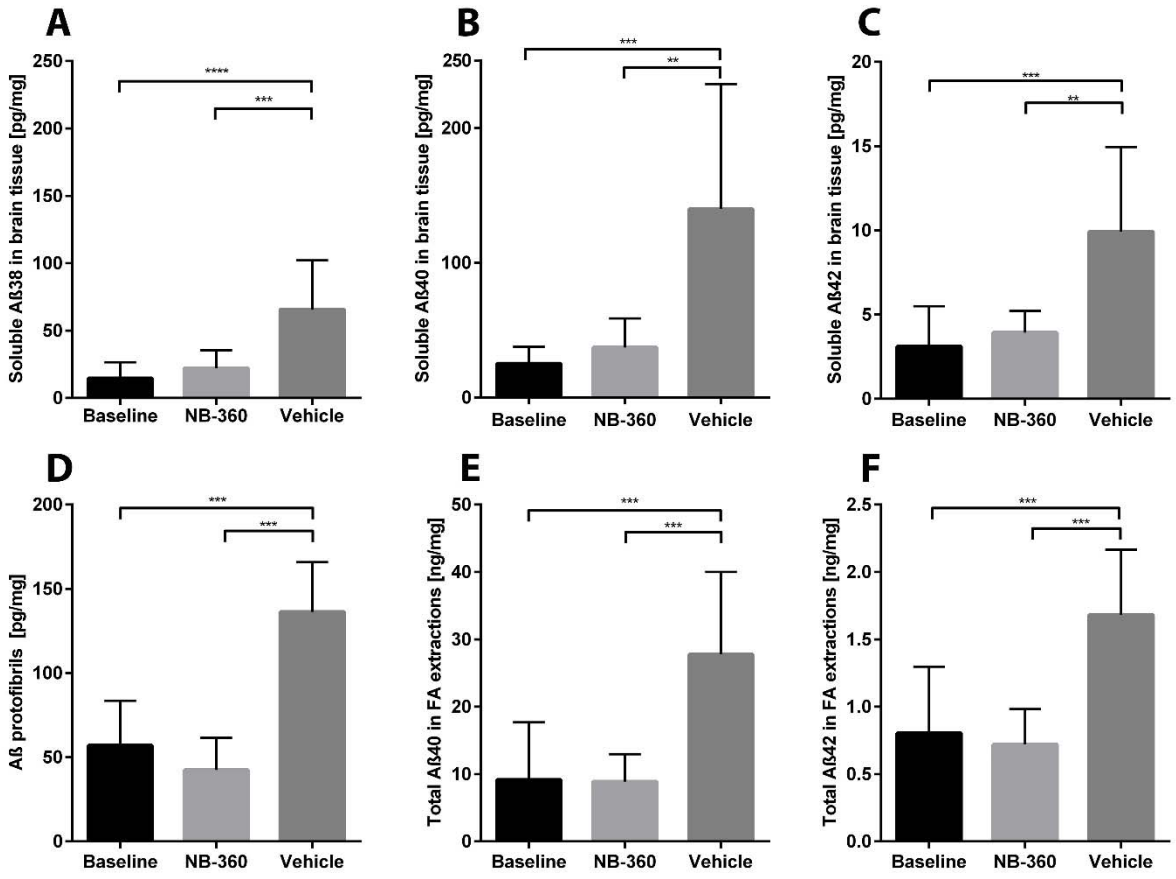

Figure 5: Aβ analysis in post mortem brain. TBS soluble Aβ38 (**A**), Aβ40 (**B**) and Aβ42 (**C**) in brain extracts from mice after PET scanning. Bars show mean of groups with standard deviation. Baseline (n=9) and NB-360 treated animals (n=9) showed significantly lower levels of all three Aβ species compared to vehicle animals (n=11); $p<0.001$). A similar pattern was revealed with the Aβ oligomer/protofibril specific ELISA (**D**) showing a significant difference between NB-360 and vehicle animals ($p<0.0001$). Also the total Aβ40 (**E**) and Aβ42 (**F**) load, measured in FA brain extracts, showed similar results.

Supplemental Material, *Meier et al.*

Methods

Brain sample preparation

After perfusion, brains were removed and dissected in half. The right hemisphere was either fixed in 4% PFA and paraffin embedded or frozen on dry ice for later autoradiography analysis. The left hemisphere was immediately frozen on dry ice for further extraction and measurement of Aβ concentrations, as previously described[15,26]. In short, brain tissue was homogenized with a tissue grinder (Teflon pestle), 2x10 strokes on ice, at a 1:5 weight:volume ratio in TBS with Complete protease inhibitor cocktail (Roche, Mannheim, Germany). 250 µl of the homogenate was mixed with another 250 µl of TBS and centrifuged for 1 h at 16000xg. The supernatants were stored at -80°C until analysis. For extraction of TBS insoluble proteins, 27 µl of the original extract and 73 µl 96% formic acid (FA) for a FA concentration of 70% were mixed for 30 s with a Kimble Pestle pellet grinder (Sigma-Aldrich, Stockholm, Sweden) followed by 1 h centrifugation at 16000xg. Supernatants were stored at -80°C until analysis.

Biochemical Aβ analyses

To break Aβ aggregates for better detection[27], TBS extracts from all transgenic mice were supplemented with 1% SDS and kept 5 min at 95°C in a compact dry heat block (Thermofisher, Sweden) and then further diluted to 0.05% SDS.

Prepared samples were analyzed with MSD Multi-Spot Assay System Aβ Peptide Panel 1 V-Plex Kit (Meso Scale Discovery, Rockville, MD, USA) for Aβ38, Aβ40 and Aβ42 using neoepitope specific antibodies to the different Aβ C-termini in combination with 6E10, which binds near the Aβ N-terminus. The assay was conducted according to the user's manual and plates were read in MSD imager (Meso Scale Discovery).

Aβ protofibrils and oligomers were measured with a homogeneous ELISA, using the Aβ N-terminus specific 82E1 (IBL International/Tecan Trading AG, Switzerland) as both capture and detection antibody and a calibration curve of synthetic Aβ protofibrils for quantification[18]. A 96-well half-area plate was coated overnight with 12.5 ng 82E1 per well, followed by blocking with 1% bovine serum albumin (BSA) in PBS. TBS brain extracts were diluted 1:25 and incubated overnight at +4°C. Soluble Aβ aggregates with a size of at least a dimer were then detected with biotinylated 82E1 (0.25 µg/ml) and streptavidin-HRP (Mabtech AB, Nacka strand, Sweden), diluted 1:4000. Signals were developed with K blue aqueous TMB substrate (Neogen Corp., Lexington, KY, USA) and read with a spectrophotometer at 450 nm.

For ELISA measurement of total Aβx-40 and Aβx-42, 96-well plates were coated overnight with 100 ng per well of polyclonal rabbit anti-Aβ40 or anti-Aβ42 (Agrisera, Umeå, Sweden), and blocked with 1% BSA in PBS. FA soluble brain extracts were neutralized with 2 M Tris and diluted 1:10000 for Aβ40 and 1:750 for Aβ42 analysis, then incubated overnight at +4°C. After incubation with biotinylated 6E10 (Nordic BioSite, Täby, Sweden) (0.5 µg/ml) and streptavidin-HRP (Mabtech AB), diluted 1:5000, signals were developed

and read as above. All sample and secondary antibody dilutions were made in ELISA incubation buffer (0.1% BSA, 0.05% Tween-20 in PBS).

Immunohistochemistry

Five µm sections from fixed, paraffin-embedded right brain hemispheres were processed with an electronic rotary microtome Hm340E (Thermofisher, Sweden). Sections were deparaffinized and incubated in 3% H_2O_2 and 10% methanol in water for 15 min. Non-specific binding was blocked with 3% BSA in PBS-Tween (0.1%) for 1 h and overnight incubated overnight with a polyclonal rabbit-anti-Aβ40 antibody (Agrisera). Sections were incubated with biotinylated goat anti-rabbit (Vector Laboratories Inc., Burlingame, CA) for 2 h at room temperature, followed by PBS washes and a 45 min incubation with Avidin/Biotin complex (Vector Laboratories). The staining was visualized by 3 min DAB development and mounted with DPX. Pictures were captured with a Nikon microscope (DXM1200F, Nikon Instruments Inc., Melville NY, USA) at a magnification of 5x and further processed with Photoshop CC photomerge to a whole brain panorama.

For Aβ and GFAP immunofluorescence double staining, sections were deparaffinized and underwent antigen retrieval in citrate buffer at 86°C for 20 min and further permeabilized and blocked for 1 h with 5% normal goat serum and 0.3% Triton-X in PBS. Aβ and GFAP were stained with 6E10 (Nordic BioSite) and anti-GFAP (Dako, Denmark), respectively. Alexa fluor 488 anti-mouse and Alexa fluor 555 anti-rabbit (Life Technologies) were used as secondary antibodies. Pictures were captured with a Zeiss confocal laser scanning microscope (LSM700) and the software Zen 2012 was used for image processing.

Tables

Table 1: Animal groups

Group		***Age***	***Number of animals***
7 month	Disease progression study	7m	n=2
10 month	Disease progression study	10m	n=2
13 month	Disease progression study	13m	n=2
16 month	Disease progression study	16m	n=3
Baseline	Treatment study, baseline group (analyzed at starting age)	10m	n=9
NB-360	Treatment study, treated group (with BACE-1 inhibitor)	13m	n=9
Vehicle	Treatment study, control group (without BACE-1 inhibitor)	13m	n=11

Figures

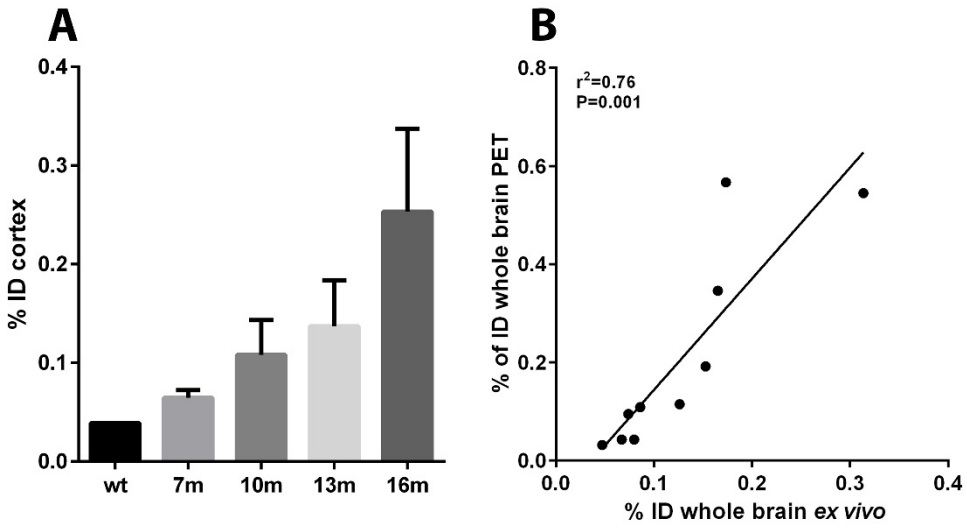

Supplemental figure 1. PET quantifiaction of disease progression and comparsion between PET and *ex vivo* activity. A. PET image-based quantification of radioactivity, expressed as %ID per gram brain tissue, in cortex of ArcSwe animals at the age of 7, 10, 13, and 16 month in comparison with old wildtype mice. **B.** Correlation of % of injected dose between whole brain PET and *ex vivo* measurements.